The r-process in supernovae with new microscopic mass formulae

Shinya Wanajo[a], Naoki Itoh[a], Stephane Goriely[b], Mathieu Samyn[b], and Yuhri Ishimaru[c]

[a]Department of Physics, Sophia University, 7-1 Kioi-cho, Chiyoda-ku, Tokyo, 102-8554, Japan

[b]Institut d'Astronomie et d'Astrophysique, C.P. 226, Université Libre de Bruxelles, B-1050 Brussels, Belgium

[c]Department of Physics and Graduate School of Humanities and Sciences, Ochanomizu University, 2-1-1 Otsuka, Bunkyo-ku, Tokyo 112-8610, Japan

We examine the effects of the newly-derived microscopic Hartree-Fock-Bogoliubov (HFB) mass formulae on the r-process nucleosynthesis and analyse to what extent a solar-like r-abundance distribution can be obtained. The r-process calculations with the HFB-2 mass formula are performed, adopting the parametrized model of the prompt explosion from a collapsing O-Ne-Mg core for the physical conditions. The result is compared with those obtained with the HFB-7 and droplet-type mass formulae.

1. Introduction

The origin of the rapid neutron-capture (r-process) nuclei is still a mystery. One of the underlying difficulties is that the astrophysical site (and consequently the astrophysical conditions) in which the r-process takes place has not been identified [11,13]. Another underlying difficulty is due to the uncertainties in the theoretical predictions of nuclear data far from the β-stability, for which essentially no experimental data exist. Recently, Hartree-Fock mass formulae with fully microscopic approaches have been constructed [3,8,4,9,5]. The latest Hartree-Fock-Bogoliubov formula, labeled HFB-2 up to HFB-7 [4,9,5], are among the most accurate mass formulae, predicting the 2135 measured masses with a root-mean-square error around 0.670 MeV for nuclei with N, $Z \geq 8$. The purpose of this study is to examine the effects of the newly-derived microscopic mass formula on the r-process nucleosynthesis and analyse to what extent a solar-like distribution can be obtained (see [14] for more detail). We adopt, here, for the physical conditions the semi-realistic astrophysical model of the "prompt supernova explosion" from the collapsing O-Ne-Mg core (see Wanajo et al. in this volume and [13]). The r-process nucleosynthesis with the HFB-2 mass formula in each outgoing mass trajectory is then calculated with a nuclear reaction network code. The mass-averaged yields over the mass shells relevant for the r-process is compared with the r-process abundance patterns in the solar system, as well as with those obtained with other mass formulae, more specifically the HFB-7 mass prediction and the extensively used droplet formulae of [6] and [7].

2. Microscopic Mass Models and the r-Process

Among the ground state properties, the atomic mass is obviously the most fundamental quantity and influences the r-process abundance predictions. A new major progress has been achieved recently within the Hartree-Fock method [3,8,9,4,5]. It is now demonstrated that this microscopic approach, referred to as HFB-2 to HFB-7, making use of a Skyrme force fitted to essentially all the mass data, is not only feasible, but can successfully compete with the most accurate droplet-like formulae available nowadays (e.g., [7]) in the reproduction of measured masses. It is found that globally the extrapolations out to the neutron-drip line of all these different HFB mass formulae are essentially equivalent. Although HFB-2 and HFB-7 are obtained with significantly different Skyrme forces (in particular, HFB-2 is characterized by an density-independent pairing force and an effective isoscalar mass $M_s^* = 1.04$, while HFB-7 has an density-dependent pairing force and $M_s^* = 0.8$), deviations smaller than about 2 MeV are obtained for nuclei with $Z \leq 82$.

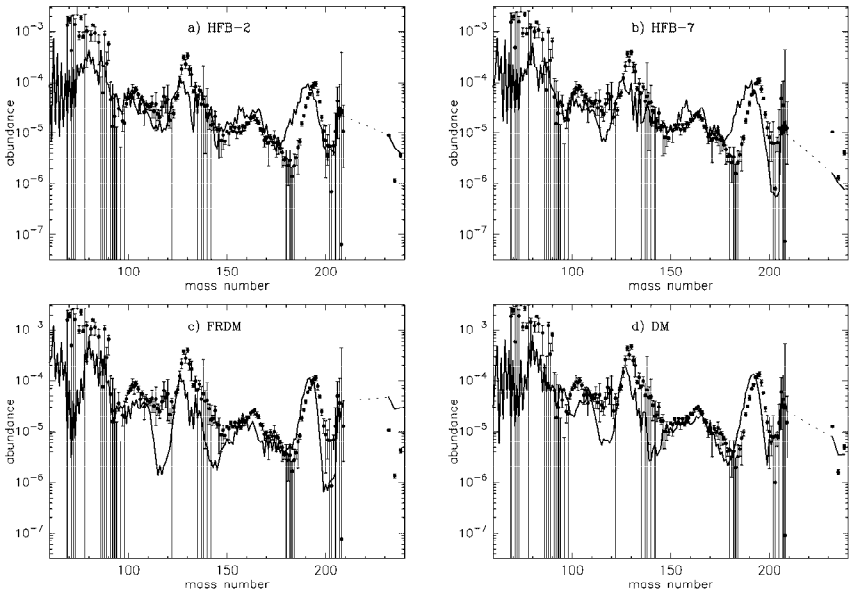

Figure 1. Final mass-averaged r-process abundances (line) as a function of mass number obtained with various mass formulae; (a) HFB-2, (b) HFB-7, (c) FRDM, and (d) DM. These are compared with the solar r-process abundances (points) from [2], which are scaled to match the height of the third r-process peak.

In the present study, we use the parametrized model of the "prompt supernova explosion" from an $8 - 10 M_\odot$ progenitor star with a $1.38 M_\odot$ O-Ne-Mg core (model Q6, see Wanajo et al. in this volume and [13] for more detail). The reason is that this model leads to r-abundance distributions that have been shown to be relatively similar to the solar distribution, at least if an artificial enhancement of the shock-heating energy is assumed. In addition, this scenario does not suffer from the problematic overproduction of $A \approx 90$ nuclei seen in the neutrino-driven wind model [15,11,12]. The r-process abundances are obtained by solving an extensive nuclear reaction network code. All reaction rates are

calculated within the statistical model of Hauser-Feshbach making use of experimental masses whenever available or the HFB-2 mass predictions [4] otherwise. The β-decay and β-delayed neutron emission rates are taken from the gross theory (GT2) [10], obtained with the ETFSI [1] Q_β predictions. Other nuclear inputs are the same as in [13].

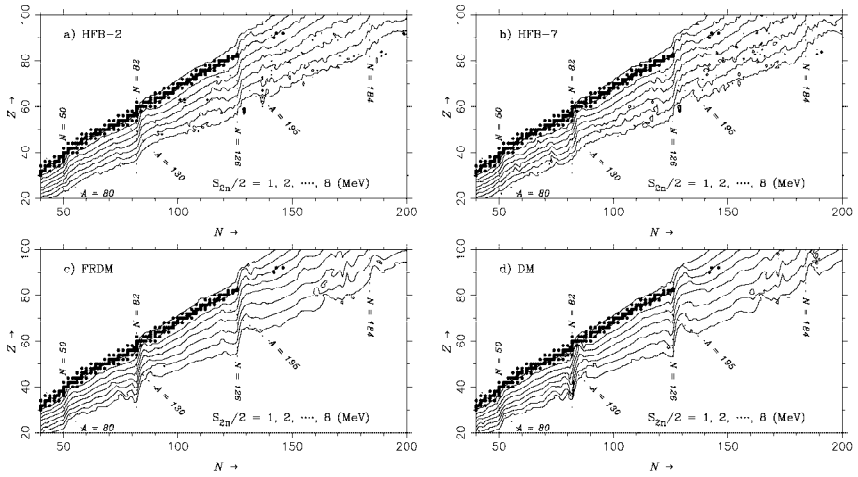

Figure 2. Contours of the $S_{2n}/2$ values (= 1, 2, $\cdots$, 8 MeV) for various mass formulae; (a) HFB-2, (b) HFB-7, (c) FRDM, and (d) DM.

3. Impact of Mass Predictions on the r-Process

In Figure 1, the mass-averaged abundances (line) are compared with the solar r-process abundance pattern [2] (dots) that is scaled to match the height of the third r-process peak. For comparison, identical calculations were performed by replacing our standard HFB-2 masses by the HFB-7 [5], FRDM [7], and DM [6] predictions. A few significant differences in the abundance patterns can be observed near the second and third peaks when use is made of the Hartree-Fock models (HFB-2 and HFB-7) on one side and the droplet models on the other side. First, the underproduction of nuclei at $A \approx 115$ and 140 is more pronounced with the FRDM and DM masses than with the HFB-2 or HFB-7 masses. Second, the abundances near $A = 130$ in the HFB cases are spread out in contrast to what is observed in the solar r-abundances. Third, the abundance curves near the third peak with the HFB masses are widened and the valley at $A = 183$ as observed in the solar r-distribution is significantly shifted to lower mass numbers. These differences reflect the model properties of iso-$S_{2n}/2$ curves (Figure 2), along which the r-process proceeds. Major local differences between the HFB and the droplet masses are found near the neutron magic numbers $N = 82$ and 126. The Hartree-Fock masses show weaker shell-closures, i.e., smoother iso-$S_{2n}/2$ curves, at $N = 82$ and 126. This reduced shell effect is responsible for spreading the second and third abundance peaks.

In order to test the impact of a change in the dynamical timescales, we modify the density and temperature profiles of each trajectory, so that $\rho'(t) = \rho(t/f_t)$ and $T'(t) = T(t/f_t)$, i.e., the dynamical timescale is multiplied by a factor of f_t. The final mass-

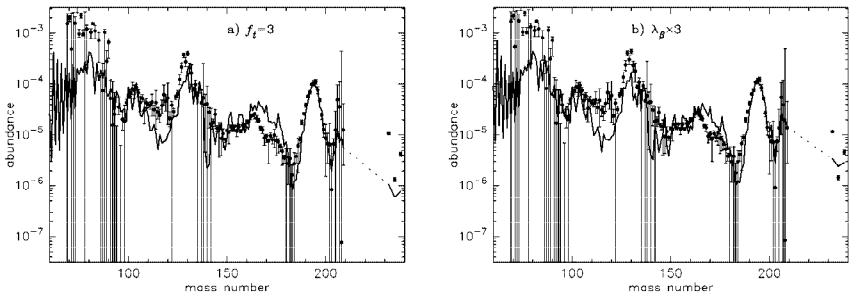

Figure 3. Same as Figure 1, but for (a) slow trajectories ($f_t = 3$) and (b) fast β-decay rates (a factor of three, see text).

averaged abundance curve for $f_t = 3$ is shown with the scaled solar r-process abundances in Figure 3a. We find a good agreement between the calculated and solar r-process patterns, in particular near the second and third peaks. However, an underproduction at $A \approx 115$ and 140 appear. Furthermore, to estimate the influence of β-decays, we show in Figure 3b the mass-averaged r-process yields obtained by multiplying all the β-decay rates by a factor of three (i.e., reducing τ_β by a factor of three). Interestingly, no significant differences are seen between Figures 3a and 3b. For β-decay rates faster by a factor of three, the freezeout (corresponding to $\tau_\beta = \tau_n$) takes place at higher temperatures and thus at higher S_a^0 value, which has globally the same effect as slowing down the outgoing material by the same factor.

REFERENCES

1. Aboussir, Y., Pearson, J. M., Dutta, A. K., & Tondeur, F. 1995, At. Data Nucl. Data Tables, 61, 127
2. Goriely, S. 1999, A&A, 342, 881
3. Goriely, S., Tondeur, F., & Pearson, J. M. 2001, At. Data Nucl. Data Tables, 77, 311
4. Goriely, S., Samyn, M., Heenen, P. -H., Pearson, J. M., & Tondeur, F. 2002, Phys. Rev. C, 66, 24326
5. Goriely, S., Samyn, M., Bender, M., & Pearson, J. M. 2003, Phys. Rev. C, 68, 4325
6. Hilf, E. R., von Groote, H., & Takahashi, K. 1976, in Proc. Third International Conference on Nuclei Far from Stability (Geneva: CERN), 142
7. Möller, P., Nix, J. R., Myers, W. D., & Swiatecki, W. J. 1995, At. Data Nucl. Data Tables, 59, 185
8. Samyn, M., Goriely, S., Heenen, P. -H., Pearson, J. M., & Tondeur, F. 2002, Nucl. Phys. A, 700, 142
9. Samyn, M., Goriely, S., & Pearson, J. M., 2003, Nucl. Phys. A, 725, 69
10. Tachibana, T., Yamada, M., & Yoshida, Y. 1990, Progr. Theor. Phys., 84, 641
11. Wanajo, S., Kajino, T., Mathews, G. J., & Otsuki, K. 2001, ApJ, 554, 578
12. Wanajo, S., Itoh, N., Ishimaru, Y., Nozawa, S., & Beers, T. C. 2002, ApJ, 577, 853
13. Wanajo, S., Tamamura, M., Itoh, N., Nomoto, K., Ishimaru, Y., Beers, T. C., & Nozawa, S. 2003, ApJ, 593, 968
14. Wanajo, S., Goriely, S., Samyn, M., & Itoh, N. 2004, ApJ, 606, 1057
15. Woosley, S. E., Wilson, J. R., Mathews, G. J., Hoffman, R. D., & Meyer, B. S. 1994, ApJ, 433, 229